REVIEW ARTICLE OPEN

Check for updates

A review on barrier layers used in flexible stainless-steel based CIGS photovoltaic devices

Sarallah Hamtaei[1,2,3]✉, Guy Brammertz[1,2,3], Jef Poortmans[1,2,3,4] and Bart Vermang[1,2,3]

Two primary engineering challenges are en route to fabricating high-performance flexible stainless-steel based $Cu(In,Ga)(S,Se)_2$ solar cells; Growing absorbers without contamination from the substrate, and providing alkali dopants to the absorber. The former is chiefly addressed by introducing a barrier layer, and the latter by post-deposition treatment or including dopant-containing layers in the stack. Here we organize these solutions and different approaches in an accessible scheme. Additionally, reports on interaction between contamination and alkali elements are discussed, as is the impact of barrier layer properties on the interconnect technology. Lastly, we make recommendations to consolidate the multitude of sometimes inharmonious solutions.

npj Flexible Electronics (2023)7:36 ; https://doi.org/10.1038/s41528-023-00266-z

INTRODUCTION

In 1974 Bell Laboratories published their pioneering work on a $CuInSe_2$/CdS solar cell device with ~5% efficiency[1], with the ~12% CIS modules of the Atlantic Richfield Company to follow in the 80 s. Still, it took the commercial market another decade to see the lights of 10 W modules[2]. The slow but steady progress though did not stop, and since the turn of millennia, American, European, and Asian research centers gradually approached and broke the 20% ceiling on cell and module levels[3]. See the review of Mufti et al., for an overview on this progress, in terms of synthesis method, doping techniques, and substrates used, and the 2020 PV technologies roadmap for key innovations in CIGS history[4,5].

Despite achieving similar performances to (multi-crystalline) Si modules, it has proved difficult for this technology to reach double-digit market shares[6]. Of the many companies and startups active in the field, only a handful have survived the harsh realities of the energy market. Nonetheless, recent developments in two areas have given the community a breath of fresh air; i) flexible (tandem) photovoltaics for ii) (extra)terrestrial applications.

On the latter note, CIGS has been positively tested under space environment for a considerable amount of time already[7]. For instance, a study by JAXA (Japanese Aerospace Exploration Agency) in 2015 suggests redundancy of glass coverage for these cells, as they do not require radiation protection. CIGS technology has also consistently shown radiation tolerance and persistent performances under low-intensity low-temperature (LILT) conditions, and they are accessible at a relatively low price compared to space-dominant III-V products[8–10].

On the former note, most notably, there have been world record series of work from EMPA, reporting CIGS on polyimide flexible substrates since 1999 (12.8%[11]), up until 2022, with a remarkable 21.38%[12] cell. Combining such high-performing devices with liberating the configuration from constrained form factors can expand the range of PV applications to various integrated solutions in, i.a., vehicles and infrastructures (VIPV and IPV, respectively). On steel substrates as well, EMPA demonstrated at lab scale an 18% CIGS device[13], while Miasolé are producing modules with power conversion efficiencies (PCE) approaching 19% already[3].

In multiple junction formats too, all thin-film light-weight tandems comprising top perovskite and CIGS bottom cells already show promising results approaching 25% PCE[14,15]. As demonstrated by Solliance and Miasolé, such tandem concepts can also be realized in flexible configurations, with ~23% efficiencies[16]. Once mature, such products could own a niche, untapped, but large markets where silicon is either unable to enter (in several space applications) due to lack of radiation tolerance or has difficulty adopting (e.g., VIPV), due to its brittleness, rigidity, and heavyweight. In fact, such flexibility, stretchability, and low weight have been the cornerstone of products in successful companies with CIGS at their business core: Miasolé, Ascent Solar, Mid-Summer, Avancis, and Sunplugged are some of the valuable players in the market, providing products suitable for (extra) terrestrial integrated applications[16–21].

Avancis has been a leader in CIS technology since 1981, with numerous world records to date, including the current $30 \times 30\ cm^2$ fully encapsulated, glass-based modules exceeding 19% PCE[17]. While not flexible per se, their light-weight products demonstrate the immense potential of the CIGS technology as a photovoltaic solution to energy demands. They cover the entire value chain of technology and offer a range of unique products. Designed and developed in Germany, their current two premium solar modules- Skala and PowerMax®, present aesthetically stunning solutions (in many different colors) for open spaces/ solar parks and building integrated/ façades. These products surpass their thin film and (poly)crystalline competition in module performance under low light and partial shadowing and are responsive under a broad light spectrum (according to the current product sheets)[22].

Ascent solar technologies is another long-standing and active player in manufacturing flexible CIGS products onto a polyimide substrate[21]. This American company has had monolithically integrated products for consumers, government, aero-/space, and, recently, agriculture industries. Such a wide range of applications comes through off-the-shelf to custom-made products, having maximum curvature radius of 3 mm, and a specific

[1]imec, imo-imomec, Thor Park 8320, 3600 Genk, Belgium. [2]Hasselt University (partner in Solliance), imo-imomec, Martelarenlaan 42, 3500 Hasselt, Belgium. [3]EnergyVille, imo-imomec, Thor Park 8320, 3600 Genk, Belgium. [4]KU Leuven, Department of Electrical Engineering, Kasteelpark Arenberg 10, 3001 Heverlee, Belgium.
✉email: sarallah.hamtaei@imec.be

power of 0.45 W/g. Their Superlight technology is suitable for high-altitude airships and drones and has actually increased flight time of unmanned aerial vehicles of Silent Falcon by 50%. Their shatterproof, high-end product offers customizable voltage functionality, which is suitable for LILT space conditions, and will be further examined in the Jupiter mission of JAXA[21].

Midsummer is the other notable front runner of flexible CIGS, which mass produces their M2-sized flexible devices on stainless-steel (SS) substrates using their flagship DUO tool. This system can remarkably produce all layers of the CIGS under vacuum and complete an entire device every 20 s, at north of 90% reduction in CO_2 footprint compared to a traditional method of panel production[23]! Primary products of this Swedish company cover building integrated PV. E.g., WAVE is a panel named after its form factor designed for curved surfaces, particularly two-barrel roof tiles. Looking at the product sheet, such discrete panels can boast twice as much specific power as conventional alternatives at a remarkable thickness of 2 mm.Miasolé is an American company with truly outstanding SS-based flexible CIGS products. Their light-weight products (< 2.2 kg/m^2) can be implemented in a spectrum of (integrated) applications, from vehicles to carports commercial roofs, and structures in high wind and seismic areas. Furthermore, a special plastic sheet coupled with an aluminum film guarantees their water vapor resistance in long service periods. Miasolé's trademark transportation-integrated solution SolarRide™ allows customers to reduce fuel consumption, emissions, and maintenance costs notably[24]. These real-world products are illustrated in Fig. 1.

These cases exemplify the reach and quality of solutions a flexible CIGS can bring to the table. On the other hand, many lab-scale device concepts are still under research to be commercialized and scaled up. This most notably includes results of TNO/ Miasolé and TNO/ KIT on flexible and rigid Perovskite/ CIGS tandems, at 26.5% and 24.9% PCEs, respectively[25,26]. Once reliably produced at a large scale, such technologies have a big potential to compete in existing markets and dominate new ones. There exist challenges, of course.

Fig. 1 Applications of different integrated PV solutions are illustrated in an urban environment. For instance, large flat infrastructures like a bridge can use conventional Si technology, building façades can equip products such as Skala and PowerMax® from Avancis[22], consumer products like a backpack can harvest energy using Ascent Solar[21] eFilm, vehicles could partially source their power from Miasolé[24] SolarRide™ and roof tiles can sport Midsummer[23] Wave, while remain aesthetically attractive.

Either tandemed with another technology or in a standalone configuration, a critical bottleneck is producing CIGS on appropriate flexible substrates and building the technology around it. In the following chapters, we discuss this matter and detail its significance. But first, we briefly address another challenge, in sustainability and environmental concerns.

Environmental concerns have been with CIGS technology since its inception, mainly targeted at its constituent elements. From the usage of heavy metals (Cd in the CdS buffer) and (H_2)Se in the early days to the scarcity of indium and gallium, which is intensified nowadays. While the two former issues have been analyzed and addressed early on, the latter two have been the Achilles' heel in promoting CIGS in this environmentally hypersensitive era. However, recent studies and design concepts has shown some ways forward. One approach is to reduce the thickness of CIGS material and develop ultra-thin absorbers at a third of conventional designs[27,28]. Another approach is to develop tandem devices, as alluded to previously. In double junction format, such devices optimally sport a narrow-bandgap bottom cell (~ 1.0 eV), partnered with a wide-bandgap top cell (~ 1.7 eV)[29], like perovskite. This indicates few choices for the bottom material, harvesting light at the near-infrared region, with a pure selenide CISe as the industry's most robust, stable, and reliable candidate[30–32]. As the name already suggests, this entails the removal of gallium, hence avoiding the Ga scarcity issues altogether. Moving to Ga-less, or Ga-back-graded structure also means exercising an even simpler development process[33,34], which both researchers and manufacturers welcome. Looking at sustainability studies on such perovskite/ CIGS tandems looks promising as well. A recent LCOE (levelized cost of energy) analysis puts such technology on par with Si and 5 percent cheaper than perovskite/ Si tandems. From a GHG (greenhouse gases) point of view too, CIGS in either tandem (with perovskite) or single junction formats beat both Si and Perovskite/ Si tandems by more than 50%[35].

Furthermore, the misconception about indium scarcity has been recently clarified in a white paper published by the leaders of the CIGS research community. In fact, 35% of predicted indium production in the EU can already secure 100 GW/year of CIGS production[36]. Such need is predicted to be order(s) of magnitude less for emerging PV concepts (tandems, concentrator-equipped micro solar cells, etc.)[37]. Going to TW-level production is of course more challenging since In is used in other PV technologies as well-in contacts and transparent conductive oxides. Therefore, a solution could be realized in In-free alternative TCOs and chalcogenide absorbers, or in certain two-terminal tandem configurations[38–40]. So, at GW-level, In supply is not an ecological issue for the CIGS industry; It is actually 'sufficiently abundant' and 'reasonably priced'[41].

On the price note, CIGS technology has been encouraging as well. The maximum manufacturing cost for rigid glass-glass CIGS-based modules in 2015 beat their predicted costs by 0.05$/W^2, with realistic roadmaps to ultimately achieve 0.26$/W in the near future[42]. The minimum sustainable price for single junction CIGS production is also on par with perovskite technology (~ 30$/W) and 0.05$ cheaper than that of crystalline Si[35]. And that is still at low production scales for rigid standalone modules and terrestrial applications. More financial margins are harvested when replacing rigid thick glasses with their thin counterparts, or flexible substrates such as SS, and moving to the space arena. However, switching to flexible substrates is rather cumbersome and requires more studies. In the next section, we evaluate the requirements behind these alternative substrates and explain the case for using SS.

WHAT ARE FLEXIBLE SUBSTRATES?

One approach to realize flexibility is to make the device on conventional rigid substrates, e.g., Si wafers or glass, and

Table 1. Comparison of coefficient of thermal expansion (CTE) in different layers.

Material	SLG	Ti	Cu	Stainless Steel (430)	Kovar (Ni/Co)	CIGS	Cr	TiN	Al_2O3	SiO_x	Mo
CTE (ppm/K)	~9	~8.5	16.5–18.5	~10.5	~6	8–9	4.9	9	6–8	1–9	4.8–5.9

Data from multiple references[50,60,75,98,136–140].

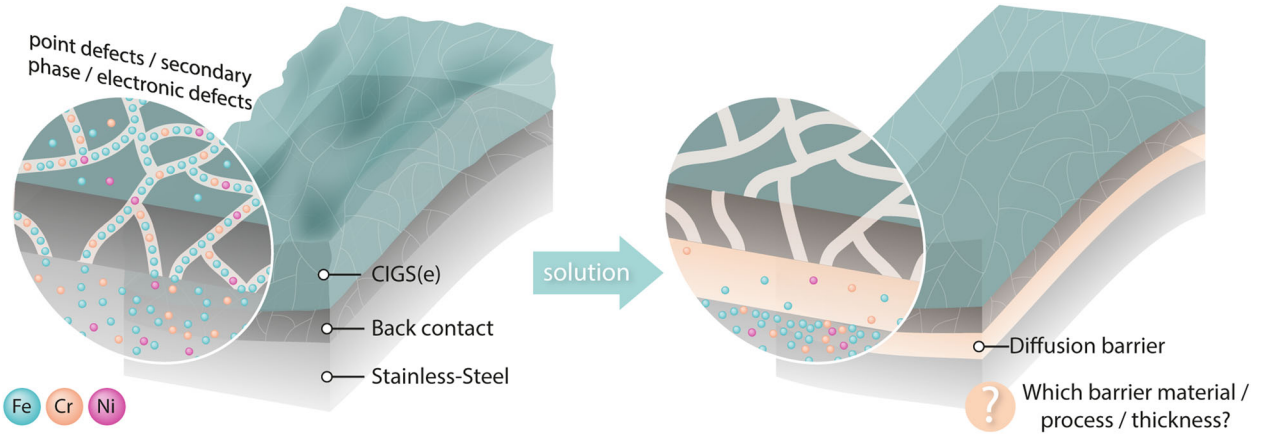

Fig. 2 Defects generation due to impurity diffusion from the substrate, and how to avoid them via a barrier.

subsequently transfer it onto bendable substrates, e.g., metallic or polymeric foils. Such a method has already been exercised in different PV technologies[43,44]. On the other hand, many research institutes and a handful of companies (as demonstrated above) have integrated flexible substrates into their CIGS process flow from the beginning, in different geometries and designs and even in stretching conditions[20,45,46].

A make-or-break part of the second approach lies in the substrate material, which must comply with many requirements[47]. From a large-scale production point of view, it should be ideally integrable into roll-to-roll processing, reasonably priced, and lightweight. Notably, it ought to be considerably corrosion resistant under exposure to chalcogen agent at high temperatures, exhibit low surface roughness, and be compatible with other layers in the stack (fits into the same thermal budget, have a similar coefficient of thermal expansion- CTE, and good interlayer adhesion)[48]. Table 1 summarizes CTE for different layers of relevance as a pivotal property.

A combination of these properties is needed to choose the substrate material. Metallic substrates are generally a practical choice due to their withstanding of the high-temperature processing conditions of CIGS absorbers (typically north of 500 °C). However, as expected, a compromise must be made as none of the candidates has all optimal properties. For instance, copper foils are interesting abundant choices, and, e.g., Solartechnik GmbH reported interesting results back in 2003[49]. However, its CTE mismatch induces poor interlayer adhesion in the stack, making the device unreliable from a mechanical integrity perspective. Mo foils are appropriate from CTE compatibility and architecture redundancy perspectives, because it is already a prevalent choice for back contact in CIGS. However, their high cost and specific weight leave them as less favorable candidates[50]. Likewise, while Ti foils meet most substrate/ barrier layer requirements, they are still too expensive to be profitable in real-world, large-scale applications- especially for terrestrial applications.

A compromise could be met in SS substrates for both terrestrial and space applications[38]. Still, the SS family has a wide variety, and the grade choice and surface preparation must also be considered. Looking at the literature, most successful cases use a ferritic 430 SS substrate; it is relatively cheap, can become very smooth ($R_a \leq 50$ nm), and has decent thermal conductivity, high-temperature resistance, and, not least, comparable CTE[50]- see Table 1.

Before processing, these substrates should be cleaned with various acids, bases, and/or organic solvents. For most of the surveyed literature here, SS is successively cleaned in an ultrasonic bath in isopropanol and acetone for at least 5 min apiece. Some also report a further bath in methanol[51], or an air baking of the SS at moderately high temperatures[52]. The cleaning procedure is intended to remove dust particles and organic and other residual surface contaminations, otherwise promoting short circuits, cracks, pinholes, and other surface-originated aberrations throughout the device fabrication phase[48].

Growing CIGS on SS involves two more critical considerations- impurity containment and stack isolation. Iron, chromium, and magnesium collectively form over 90% of SS chemical composition. However, they are known to have a detrimental impact on CIGS absorbers, especially in the case of Fe, and not least on the eventual device's short circuit current[53]. In fact, Fe concentrations at percent scale already form $CuFeSe_2$ or $FeInSe_2$ compounds and damages the absorber function[54,55]. Studies have shown that the Fe presence beyond 30 ppm level reduces the charge carrier collection in the absorber- especially in the NIR region, decreases the net doping concentration and/or induces defects that hinder carrier mobility in the CIGS layer[53,56,57]. This problem is illustrated in Fig. 2. This critical threshold is suggested to be as low as sub-ppm levels to achieve 20% CIGS solar cells. Alas, once inside the absorber, the Fe diffusion kinetics in CIGS results in its even distribution across the depth of the film very quickly[58], thus defecting the entire film.

There are two main approaches to address this problem. Lowering the thermal budget in absorber growth stage can reduce the chance of outward diffusion of these elements from the SS substrate, as shown before[57]. However, such has unwanted side effects; Indeed, high-temperature processing is either integral to the process (in a two-step sequential method) or remarkably beneficial (in the co-evaporation method) in

Table 2. A summary of metallic barriers used in SS-based CIGS.

Substrate	Barrier	Thickness (μm)	Depo. method	Absorber process	Temp (°C)	PCE (%)	Source
$SS^{Mild\ Tata}$	Ni+Cr	2 + 0.1	electro plating	multistage	400–550	18	13
SS	Cr	0.076	e-beam evap.	multistage	550	13.82^{+NaF}	82
SS		0.2	e-beam evap.	sequential (Se)	550	$_{Kesterite}4.8^{+NaF}$	51
SS		0.1-0.2	evaporation	sequential (Se)	550–620	8.7	49
$SS^{Austenitic}$		0.22	DC	sequential (Se)	450–550	$_{Kesterite}3$–3.5	81
SS		1	DC	sequential (H_2Se)	500	9.9	141
SS^{430BA}		0.07-1	DC	3-stage	330–570	~9	84
SS		-	x	3-stage	x	17.7^{+NaF}	142
SS^{430}		0.2	x	co-evap	500–520	14.1^{+NaF}	83
SS^{430}		0.1	x	multistage	425–525	14.1^{+NaF}	57
SS^{Mild}	Mo	0.5-2	DC	1-stage	>600	$(6.2–11.4)^{+NaF}$	54
$SS^{Ferritic}$		2.7	DC	1-stage	~600	$10.3^{+RbF\ PDT}$	75
SS		0.8	RF	3-stage	400–480	12.2	50
SS^{304}	Mo: Na	0.6	DC	3-stage	-	12.03^{+Na}	78
SS^{304}		0.6	DC	3-stage	300–550	8.73^{+Na}	79
SS^{430}		0.9	RF	3-stage	400–750	15.04_{+MgF2}	77
SS^{461}	Ti	0.05	e-beam evap.	x	550	x	62
SS^{430}		0.2	RF	1-stage	540	12.9	90
SS^{430}		0.05	DC	sequential (S)	560	4.10^{+NaF}	87
SS^{430}		0.05	DC	sequential (S)	560	$6.29^{+Mo:Na}$	88
Fe	Ti-W	0.3- 0.5	DC	x	673-823	x	73

DC and RF indicate direct current and radio frequency sputtering, Also, depo, temp, SS^{x}, and x, denote respecitvely, deposition, temperature, stainless-$steel^{grade}$, and not mentioned or not carried out.

obtaining ideal roughness, grain growth and phase transformation in CIGS synthesis.

To avoid such compromise in the thermal budget, either a defect passivation technique should be implemented, as demonstrated lately by Ag alloying[59], or more commonly, a diffusion barrier can be deposited to block the out-diffusion of substrate impurities in the first place. A barrier could ideally have insulating properties as well to accommodate monolithic integration technology. This unification of barrier properties would reduce at least one process step to help simplify the manufacturing steps. Once a fully functioning barrier, complying with all the requirements, is in place, the rest of the stack could be developed in iterations and following the footsteps of rigid CIGS technology development. For a hallmark in studying flexible SS-based CIGS, readers are encouraged to see the works of ZSW[60,61]. In this context, the next chapter looks at different types of barriers in literature and discusses their performance.

WHAT ARE THE CHOICES FOR DIFFUSION BARRIERS IN SS-BASED CIGS?

Both diffusion and insulation properties of the barrier(s) used are mainly a product of their type (material), thickness, synthesis method, and the deposition technique of the subsequent layers in the stack[55,60]. Above all, barriers' adhesion, and surface properties (under all processing steps) are essential for the device's mechanical stability and integrity. This becomes particularly critical in the case of large-scale modules where there is a higher probability of defect generation in the layers. E.g., enamel layers with thicknesses beyond 10μm exhibit decent insulation and diffusion properties but lack the desired mechanical properties[55]. On the other hand, implementing a barrier may necessitate adjustments in other layers of the stack. For instance, Morán et al. demonstrated how different types of barriers could remarkably change Mo back contact's microstructure, adhesion, thermomechanical stability, and volatility under high processing temperatures- properties that eventually affect device performance[62,63].

Lastly, unlike soda lime glass (SLG), SS substrates are devoid of alkali elements by nature. Therefore, automatic inclusion of these elements via outward diffusion from the substrate during growth phase is not possible. As such, the heights of SLG-based technology cannot be achieved unless other strategies are followed to include these alkalis. Three primary techniques include PDT (post-deposition treatment), adding an alkali-containing precursor layer, and added functionality to the back contact or the barrier layers[48,50,64]. Furthermore, depending on the technique and whether light or heavy alkali is used, their impact might vary considerably[65]. For more details on these strategies, readers are encouraged to see the exceptional review from INL and HZB[66].

All these considerations have led different groups to develop various barriers, which can be classified into metals, nitrides, oxides, and alloying techniques. Tables 2–4 encompass a collection of contributions worldwide, including a few entries of Kesterite and CdTe literature- this can be relevant as the materials, processing techniques and temperatures are comparable to that of CIGS. The following sections will cover notable instances of metallic, nitride, oxide, and other unclassified barriers. Also, alkali elements inclusion and their interaction with the barrier layer's performance are discussed when relevant.

Unclassified

There have been reports with no notion of barrier layers. These are indeed interesting results but are pretty rare as far as our surveyed literature goes. This might suggest that a barrier was indeed used, but only not explicitly discussed. The most notable case is the work of NREL in 1999, when Contreras et al. reported an impressive 17.4 CIGS on SS (with anti-reflection coating),

fabricated by a modified 3-stage co-evaporation method[67]. Comparatively low but still remarkable results for barrier-less devices were achieved by Satoh et al. and Kampmann et al.[49,68]. In the latter case, contrary to the expectations, they found traces of iron only in samples with as thick as 100–200 nm Cr barriers, compared to no barrier. Which suggests either the barrier actually facilitated the diffusion, or it wasn't free from iron in the first place. On the sequential selenization route, Jung et al. published on 11.45% efficient SS-based CIGS devices with no reported barrier[69]. Their solution processed alkali doped absorbers showed smooth, coherent microstructure but fell short in terms of minority carrier lifetime. A very remarkable contribution can also be found in a report by Institut für Physikalische Elektronik, where instead of a barrier to block impurities, an etching treatment (with e.g., KCN) is advised at the CIGS/ CdS interface, to produce highly efficient devices[70]. On pure sulfide CIGS front too, very decent devices were reported by Dhere et al., with sometimes no mention of barriers[71]. Another notable example in unclassified barriers are high-temperature-resistant polymer-derived ceramics which found their way from the ceramics world to CIGS technology[72].

Metals

Metals are interesting choices of barriers due to their excellent thermal conductivity and general resistance at high temperatures. Additionally, their combinations and alloys open a vast horizon of possibilities. E.g., Gao et al. presented an in-depth study on a W-Ti alloy to block iron diffusion. In studying the kinetics of the Fe diffusion, they found a layer of ~300 nm thickness to be effective in keeping Fe away from CIGS. Furthermore, they identified grain boundary diffusion as the primary mechanism for Fe atoms to diffuse inside their barriers[73]. To avoid this, Kumar and Avashti deposited high entropy alloy nano-crystallites in an amorphous matrix (to minimize grain boundaries) and indeed saw no penetration of Fe into the barrier under very high anneal temperatures[74]. However, their performance under a chalcogen atmosphere was not investigated. Besides these rare cases of alloys, pure Mo, Cr, and Ti have been commonly used as barriers. These are summarized in Table 2, and notable examples are covered afterward.

A rather intuitive approach to block the impurities from the SS substrate is to extend the thickness of (Mo) back contact. In their enlightening work, Wuerz et al. investigated the iron diffusion in CIGS grown on mild steel and observed a logarithmic dependence of all cell parameters on the thickness of the Mo layer- with the highest impact on the short-circuit current density[54]. Curiously, on a Moly back contact/ barrier layer of ~550 nm, which lies within typical thicknesses used in the literature, they could deduce 170–381 ppm concentration for Fe atoms- a hundred times more than the critical value. Therefore, they concluded that to keep the concentration under an acceptable threshold and achieve world-class devices, a minimum 2 µm thick Mo back contact is necessary. Still, pondering these conclusions in light of their applied CIGS processing method (1-stage co-evaporation) and substrate (mild steel) is worthwhile. This Mo thickness suggestion was picked up in ZSW's subsequent work in 2017, where they looked for the locale of Rb activity in CIGS co-evaporated on SS at 600 °C substrate temperature[75]. Rubidium was introduced to the system by evaporating a RbF layer onto the CIGS layer before annealing the stack in vacuum at 355 °C for 20 min. In their thorough investigation, Rb was not detected in the grain interior (< 0.015%). Instead, high-angle GBs, dislocation cores, and the CIGS/$MoSe_2$ interface were identified as favorable diffusion paths (and passivation targets) of Rb[76]. Understanding this is particularly important because, as seen in other works, Fe diffusion is also more likely through GBs of the barrier or CIGS[75].

Another approach to include alkali is to use a sodium-doped Mo layer beneath a conductive Mo layer. As demonstrated by different groups, such a bilayer structure provides both a Na reservoir and a diffusion barrier property while serving as the electrical back contact[77]. Like in rigid devices, alkali elements, such as Na, have been demonstrated to positively impact the SS-based CIGS through structural, compositional, electrical, and texture avenues[78]. Therefore, while including light or heavy alkalis seems beneficial, its simultaneous optimization with diffusion blockage properties is necessary. Such consideration becomes even more critical when the interaction of alkalis with Ga grading, CIGS spectral response, and $MoSe_2$ layer formation is also taken into account[79,80].

Chromium is another metallic layer broadly used as a barrier layer due to its suitability under more corrosive and thermally intense environments[51,81]. Using Cr barriers at sub-100 nm thicknesses, a few groups successfully developed highly efficient solar cells[57,82].

Ångström Solar Center studied the interplay of a Cr barrier and NaF alkali layer, both deposited at the Mo interface of a co-evaporated CIGS. At low Cr thicknesses, (excess amount of) NaF appeared to negatively affect the device by facilitating the Fe outward diffusion[83]. HZB and ZSW also followed the same idea with 100 nm of Cr and 8 nm of NaF for co-evaporated CIGS and could achieve same performances at a lower maximum growth temperature (425 °C). At the same thickness, they could reduce Fe concentration in the absorber to below 80 ppm. Later, Cho et al. actually established a positive correlation between Cr barrier thickness and device efficiencies[84]. An attempt which was made by Kampmann et al. a decade earlier, though not conclusive[49]. In any case, too much thickness imposes its own challenge by promoting (extra) Cr accumulation at the Mo interface and deteriorating the back contact[83], or positively affecting Fe concentration[49]. Thus, applying Cr-barriers and alkali reservoirs together needs careful co-optimizations, as was seen in Mo barriers.

A Cr/Ni bilayer was also recently shown by TNO at WCPEC-8 conference to effectively impede Fe, Ni, and Cr concentration in CIGS to below three ppm (per Secondary ion mass spectrometry-SIMS). Their reported 17.9 PCE device was co-evaporated at 550 °C and had a double Mo: Na/ Mo: K alkali source sandwiched between the absorber and Mo back contact. The combination of Na and K could achieve slightly higher V_{OC} than Na alone. EMPA also used a similar Ni-Cr barrier layer for their certified world-record CIGS device in 2018 (on mild steel). While Ni trace was found in their absorber, it could not be associated with defects identified under admittance spectroscopy. Instead, Cr and/or Fe impurities could be linked to a non-radiative recombination center around 0.33 eV, whose formation their barrier could impede in a CIGS grown under 500 °C. They demonstrated that going to higher substrate temperatures, while still succeeding in reducing the formation of such defects, requires an extra TiN barrier[13]. This will be more discussed later in the nitride section.

Titanium has been also used as a flexible substrate to CIGS for a long time[85,86]. Though here, we only cover the literature reporting it as a barrier layer on SS. In two subsequent works, UNSW researchers worked on 50 nm Ti barriers to synthesize SS-based Kesterite in a two-step sequential sulfurization route. Mainly, they experimented with different sources of Na to assess its impact on, i.a., the elemental distribution of absorbers and impeding the substrate impurities[87,88]. In one work, the sodium was supplied by evaporating a NaF layer onto the metallic precursor, while the other implemented different configurations of Mo: Na and/or Mo as their back contact. Their study shows poor adhesion and uniformity when the absorber directly interfaces a Mo: Na layer in all configurations, as previously seen in CIGS literature as well[89]. Such an issue was shown to be resolved by sandwiching as thin as 30 nm conductive Mo between the absorber and Mo: Na layers. Furthermore, all other barrier/ back contact configurations with Ti/ Mo and Mo: Na showed excellent Fe and Cr blockage to below

Table 3. A summary of nitride barriers used in SS-based CIGS.

Substrate	Barrier	Thickness (μm)	Depo. method	Absorber process	Temp (°C)	PCE (%)	Source
SS	Ti/ TiN	0.06/ 0.23	Pulsed DC	PVD	350–435	$_{CdTe}10.9^{+Cu}$	92
$SS^{NK\text{-}430MA}$		0.05/ 0.3	Reactive RF	3-stage	350–550	8.9^{+MoNa}	99
SS^{Mild}	TiN	0.35	DC	x	700	-	100
Ti		0.05	Sputtering	sequential (Se)	580	4.85	96
SS		0.02-0.1	Sputtering	x	700	x	93
Glass/ Si		0.5	Reactive Sputtering	x	-	x	104
SS^{316}		0.07/0.35	RF	x	450-550	x	98
SS	CrN	1	E-beam evap.	3-stage	550	9.8	82
SS	AlN	0.2-1	DC	3-stage	530	11.8	106
SS^{430}	AlN, Si_3N_4, Al_2O_3	0-3	Doctor blade	x	600	x	107
SS^{430}	Mo_xN_y	0.8	RF	sequential	550	6.86	110
SS		0.6	Reactive Sputtering	closed space sublimation (CSS)	400-500	x	91
SS	Si_3N_4	1	PECVD			x	
$SS^{430,\ 316}$		0.5	RF	CSS	400-650	$_{CdTe}6.2$	109

DC and RF indicate direct current and radio frequency sputtering, Also, depo, temp, SS^{x}, and x, denote respecitvely, deposition, temperature, stainless-$steel^{grade}$, and not mentioned or not carried out. Note that PECVD indicates plasma-enhanced chemical vapor deposition.

sputtering target material impurity of 10 ppm[88]. However, they report a slight accumulation of Ti at the bottom of the absorber, the effect of which required further investigation. Regarding the elemental distribution, either NaF or Mo: Na alkali sources showed almost always a correlation between sodium and oxygen depth profiles (according to time of flight- SIMS). Moreover, NaF addition could counter metallic elements segregation otherwise present in the absence of sodium[87], while Mo: Na source did not result in a typical U-shaped Na profile (which is understood as beneficial in their SLG-based CIGS)[88].

Another point of interest raised by Jiang et al. in using Ti is its texture's impact on suppressing impurities. They identify granular structure, voids, and dislocations associated with a dominant (002) crystal orientation as primary diffusion paths for Fe atoms in the Ti. Instead, a (001) dominated texture, realized under lower sputtering pressure, provides a smoother surface with more efficient blocking[90]. Furthermore, while such a Ti barrier looked necessary (and successful) to impede Fe and Cr, it was redundant to block Ni impurities from SS. Indeed, only the triple layer of Mo back contact used in their stack was found sufficient to block Nickel.

A common theme in most Ti literature is the adhesion it provides to the whole at the SS substrate interface. This is unsurprising given its compatible CTE[85] (8.6 ppm/K) with the rest of a typical CIGS stack- see Table 1. As will be seen, this adhesion improvement is a feature other groups have tapped into to realize or improve oxide-/ nitride-based barriers.

Nitrides

Different nitrides have been widely used in semiconductor technology as impurity barriers due to their high thermal, chemical, and mechanical stability, hardness, melting points, and resistance to moisture corrosion and mobile ions diffusion[91]. Therefore, many groups have tried to use them as a barrier and/ or an insulation layer in SS-based chalcogenide thin film solar cell technologies. Table 3 summarizes some of these work, with occasional entries on Ti, Si, and glass substrates.

Titanium nitride has been successfully implemented to block diffusion from SS in other technologies with similar processing temperatures, i.e., CdTe PV and Bi_2Te_3 thermoelectrics[92–94]. In the case of CIGS, its similar CTE helps avoid thermal stress-induced damages at high temperatures, which in turn helps crystal growth and avoids layer detachment. Furthermore, TiN's high thermal stability and high optical reflectance in the NIR region have made them the most applied nitride barrier in the literature of SS-based CIGS[93,95].

In a study of sequentially grown Kesterite, Sun et al. investigated the TiN thickness effect on residual stress in the absorber layer; a 75% stress relief was seen when using 100 nm of TiN (instead of none) beneath their Ti-based Kesterite[96]. Additionally, TiN introduction could result in higher crystalline quality with less porous microstructure (by a factor of 4), hence higher compactness and mechanical stability under bending conditions.

A relatively thin Ti layer beneath the TiN can improve the adhesion at the SS interface, as seen in other applications[97]. Such Ti layer also alleviates the roughness of SS and, in turn, helps with the diffusion properties via improved microstructure/ texture[98,99]. Liu et al. worked on Ti/TiN and evaluated their stacking configuration effect on Fe blockage through roughness, texture, and depth composition analysis[99]. In their CIGS device stack, they used a triple layer of Mo back contact and compared a multi-layer versus bilayer barrier of Ti/TiN with an overall equal thickness; The multi-layer comprised many Ti interlayers, which eventually resulted in a smoother surface. However, this did not translate into improved Fe blockage than the bilayer counterpart as the TiN thickness and crystallinity were reduced. Still, the interaction between these effects is confounded and not perused in the paper.

The sole effect of TiN texture on Fe and Cr blockage was investigated later by Kumar et al. on a similar bilayer configuration[100]. By modulating the sputtering conditions, they controlled the preferred orientation of TiN films deposited onto SS; Under an annealing temperature of 700 °C, they found films oriented at (111) to show little grain boundary diffusion of Fe ions (contrary to Cr) and reported a remarkable diffusivity of 1.5×10^{-18} cm^2/s[100]. However, results should be treated with care due to the absence of Se or S in their annealing atmosphere.

A point of consideration for (Ti/) TiN barriers is their relatively high electrical conductivity[101], which removes the option of monolithic interconnection. An additional insulating layer, such as SiN_x could overcome this. Still, when used in advantage, the high conductivity of TiN might actually help reduce the back contact thickness in the stack (or even its omission), hence reducing the costs. There is actually a strong case for the potential of TiN, as its average work function is close to that of Mo[102,103]. Attempts to practice such an idea on Si and glass substrates have been

Table 4. A summary of oxide barriers used in SS-based CIGS.

Substrate	Barrier	Thickness (μm)	Depo. Method	Absorber process	Temp (°C)	PCE (%)	Source
SS	Cr_2O_3	x	Annealing	sequential (Se)	500	5.86	116
SS		x	Annealing	sequential (Se)	500	10.6	117
SS	Fe_2O_3	0.012	Annealing	sequential (Se)	500	10.15	115
SS^{430BA}	iZnO	1	RF	3-stage	350–590	13.95^{+Na}	133
SS^{430}		0.2	RF	3-stage	540	12.5	131
SS^{430}		0.1– 0.2	RF	3-stage	x	x	143
SS^{430BA}	ZnO	0.05	RF	annealing	550	x	62
SS		0.05–0.2	RF	3-stage	500	9.06	134
SS^{430}		0.5	RF	sequential (Se+ H_2S)	480	10.3	121
SS		1–3	DC	3-stage	570	10.04^{+Na}	135
SS		1.5	Sputtering	3-stage	350-550	15	144
SS	Al_2O_3	0.1–1	SPD	3-stage	475	14.4	127
SS^{430}		25 + 10	Anodization	$3\text{-stage}_{submodule}$	500	15.9	132
SS^{430}		0.3	ALD	3-stage	540	$\sim 13.44^{+Na}$	131
SS		0.1–0.3	ALD	Co-evap	550	x	129
SS^{430}		2	RF	3-stage	400-540	15.8^{+Na}	145
SS		0.15	RF	3-stage	500	x	146
SS	SiOx+Al_2O_3	10	Silk screen printing	3-stage	580	10.2	147
$Ti,SS^{Kovar,\ Cr}$	SiOx, Al_2O_3	1–3,3–7,1–6	RF, Sol-Gel, PECVD	x	500-600	10.8, 10.7, 10.9	55
$SS^{Kovar,\ Cr}$	SiOx (:Na)	1.5-3	PECVD | Sol-Gel	Co-evap	550	12.3^{+Na}	48
SS^{Sheet}	SiOx (:Na)- Enameled	3.4	PECVD | Sol-Gel	1-stage	600	12.8^{+Na}	53
SS^{Mild}	Enameled	150	Spray coating	multi-stage	600	$17.6^{+Na+K}{}_{+MgF2}$	125
$SS^{Enameled}$		x	Spray coating	$x_{Submodule}$	-	15.4_{MgF2}	126
Ti	SiOx	3	$PECVD^{microwave}$	1-stage	550	14.1^{+Na}	148
SS		3	PECVD	3-stage	-	10.57^{+Na}	119
SS^{430BA}		1	PECVD	3-stage	350-590	11.82^{+Na}	133
SS^{430BA}		2	PECVD	3-stage	-	12.43^{+Na}	120
SS^{430}		0.5	PECVD	sequential (Se+ H_2S)	550	$_{Kesterite}10.3^{+NaF}$	121
SS^{430BA}		0.2	DC	3-stage	360-560	15.6	123
SS		x	x	multistage	450-580	19.1^{+RbF}	149
SS^{430}		0.2-0.6	SPD aerosol	x	500	x	122
SS^{316}		2, 1.5	Sol-Gel, Sputtering	x	500	x	63
SS^{430}		1	Sol-Gel	sequential (Se)	540-570	3.8	52
SS		1.5	Reactive sputtering	CSS (CdTe)	390-420	x	91
SS		1	Silk screen printing	3-stage	580	10.57^{+Na}	147
SS		0.3	RF	3-stage	500	12.3	146
SS^{304}	Ti+SiOx/AlOx	0.6 + 0.25/2	Pulsed DC	x	500-700	x	124

DC and RF indicate direct current and radio frequency sputtering, Also, depo, temp, SS^{x}, and x, denote, respecitvely, deposition, temperature, $stainless\text{-}steel^{grade}$, and not mentioned or not carried out. ALD and SPD, indicate atomic layer deposition and spray pyrolysis deposition, respectively.

made[104], while others actually utilized TiN as a back contact concept in CIGS solar cell processing/ operation[98]. Such an idea is also seen in other nitrides like CrN[82]. However, they observed a V_{OC} lower than expected in achieving cells just shy of 10% efficiency. This subpar performance was traced back to defects generated in the CIGS absorber due to Fe and Cr diffusion from the substrate or barrier/ back contact, respectively. Therefore, simultaneous optimization of conductive nitrides as both back contact and diffusion barrier requires more meticulous research.

Another nitride of interest is the insulating AlN which has a similar lattice constant and CTE (4.2 ppm/K) to Mo (4.8 ppm/K)[105]. Li et al. illustrated the efficacy of a micron-thick AlN layer to block impurities, improve Mo microstructure, and insulate the stack from SS in CIGS PV[106]; They report on the necessity of going beyond micrometer thickness for AlN in order for the sputtered film to sustain its insulation properties and resist peeling off under scotch tape tests. Furthermore, the barrier improved Mo microstructure through grain enlargement- without detrimental impact on Mo crystallinity, but at the expense of a slight increase in root mean square roughness (~ 1.5 nm)[106].

Delgado-Sanchez et al. focused on developing adhesive AlN barriers with high throughput and less costly methods, i.e., doctor blading using various aqueous suspensions comprised of Al_2O_3, AlN, and Si_3N_4 powders, as well as additives[107]. In their investigation, solution-processed bilayers of either Al_2O_3 or AlN resulted in a reduction of 52% in surface roughness and absolute values lower than sputtered Al_2O_3. Both configurations with a similar overall thickness (~ 1.3 μm) also showed no signs of cracks or layer detachment incidence under high-temperature treatments (after barrier deposition); they both showed decent

insulation measures and succeeded in preventing Fe diffusion according to X-ray photoelectron spectroscopy analysis[107].

Molybdenum nitride is also a potential barrier candidate coming from the Cu metallization practice in semiconductors[108]. Palekis et al. observed the superiority of Mo_xN_y diffusion barriers compared to Si_xN_y, in CdTe devices[91,109], not least in the interlayer adhesion, given the difference in CTEs[109]. In CIGS, Li et al. sandwiched a fixed thickness of Mo_2N between an adhesive and conductive Mo. In doing so, they found no impact on the crystalline quality of conductive Mo or the absorber layer. Furthermore, while they succeeded in dramatically reducing Fe outward diffusion, their device only shows modest PCEs. This was attributed to the selenization nature (sequential method), suboptimal barrier thickness (hence Fe diffusion), and, not least, lack of alkali doping[110]. All of which indicate a need for more studies.

Oxides

Oxides are commonly used in semiconductors for different purposes, including passivation, isolation, and impurity barriers[111]. Therefore, their application in PV technologies is understandable[112,113] as their properties are known and widely researched. Table 4 summarizes notable uses of oxides as a barrier for CIGS, Kesterite, and CdTe devices. Such oxide layers could either be made via direct deposition or through the oxidation of specific materials. Many groups also tapped into the dielectric properties of oxides and evaluated their insulation performance. Some of these are also covered.

Researchers of Chonbuk National University in Korea have produced some limited resources available on flexible SS-based CIGS devices made via a sequential two-step technique. In this method, a metallic precursor of the constituent elements is selenized (and/or sulfurized) in a selenium (and/or sulfur) containing atmosphere. Although holding the higher promise of large-scale manufacturing (compared to, e.g., co-evaporation), this method is known with Ga accumulation at the Mo interface and hence, creating an inconsistent bandgap throughout the bulk[114].

In order to address this issue and promote a coherent, uniform CIGS absorber, Lee et al. suggested using a Se interlayer in their metallic stack[115]. Then, a homomorphic barrier was grown on the SS substrate by its oxidization at 600 °C for a single minute. This work reported this process to result in a Fe_2O_3, and a Cr_2O_3 in their later publications[116,117]. Either way, they report the remarkable efficacy of such barriers in blocking Cr contaminations and smoothening the SS surface. However, while Fe inclusion is significantly limited, its trace was not negligible[116].

Silicon dioxide and its variations are unsurprisingly the most employed (oxide) barrier layers. Also used in other fields as an insulating layer[112], their nitride variation is actually widely present in glass-based CIGS stack, to i.a., block diffusion of native alkalis[118]. ZSW published one of the detailed systematic studies of dielectric barriers for fabricating flexible CIGS modules on Ti, Kovar, and Cr-steel foil substrates, focusing on silicon (di)oxide[55]. They found evidence for interactive effects of the barrier's deposition technique and thickness on its dielectric and adhesion properties.

Concerning the surface and interlayer properties, combining specific deposition techniques can aid in minimizing barrier surface defects and roughness. E.g., SiO_x via sol-gel[52] or PECVD were shown to improve the surface roughness; 2 and 3 µm SiO_x and SiO_2, respectively, doubled down the surface roughness[119,120] and thin enough amorphous SiO_x also smoothed the surface and was suggested to be (more) successful in blocking the Fe diffusion[121,122], probably due to lack of grain boundaries. Still, the thickness impact is not linear and might affect other properties. Less than a threshold might result in delamination (e.g., 3 µm for sol-gel deposited SiO_x) or inefficient contamination blockage[68]; Exceeding a certain thickness causes pinholes and cracks and reduced flexibility, though improving the dielectric and diffusion properties (e.g., more than 10 µm in high-temperature varnishes and enamel layers). Another concern for higher thicknesses is the cost of material and processing time, especially when made via sputtering[123]. Depending on the synthesis method, different thicknesses are reported to be a practical compromise; ZSW suggests 3 µm double layer SiO_x, SiO_x: Na, made via PECVD and sol-gel, respectively, while 200 nm was suggested for sputtering or aerosol deposition[48,122,123]. Adding an adhesive Ti layer beneath the former (also seen elsewhere[124]), together with co-deposition of NaF, improved SS-based device performances and interlayer adhesion, as documented in the exceptional work of Wuerz et al. [53].

To study dielectric properties on either Ti, Kovar, or SS substrates, Herz et al. demonstrated the necessity of tests under real CIGS synthesis conditions[55]. That is, characterization after mere high temperature treatment might lead to unreliable conclusions, and exposure to the chalcogen agent is essential to the analysis. After such rigorous testings, beyond 60 V breakdown voltage was achieved through a combination of barriers; 6 um thick bilayers of SiO_x, prepared through CVD and sol-gel techniques, respectively, as well as a combination of PECVD deposited SiO_x with RF sputtered Al_2O_3. However, single layers of either kind didn't fare as well. This is in part because the additional layer helps with both insulation (partially through layer thickening), and reduction of pinhole densities. It is certainly plausible to assume impact of the latter on the former. This observation is also reported elsewhere when using multiple layers of SiOx and AlOx. Nevertheless, given the lack of actual testing after exposure to CIGS growth conditions, results should be seen carefully.

ZSW also demonstrated the efficacy of enameling as a multifunctional, high-temperature resistant layer, an alkali source for CIGS, and an insulation and diffusion barrier. Indeed, the 130 µm enamel layer limited Fe atoms by a factor of 300 to unharmful levels (compared to when it is not used), insulated the stack with no signs of microstructural flaws, and provided sodium and potassium concentrations and profiles comparable to (or even better than) glass-based technology. The technique was also used to produce 10×10 and $23 \times 30\ cm^2$ modules with a remarkable 14.5% and 12.9% efficiency, respectively (without antireflective coating)[125,126].

Aluminum and (intrinsic) zinc oxide are other choices of barrier layers due to their attractive properties, including matching CTE, thermomechanical stability, chemical inertness, thermal conductivity, and high insulation[127]. Above all, these layers are already integrated into CIGS production; Al_2O_3 has been a choice of back surface passivation[128], while ZnO has been the stack's most commonly used buffer/ window layer. Therefore, their usage makes the process flow in the fabrication procedure less complex.

Al_2O_3 is used as a standalone or in combination with SiO_x. Park and Bae et al. focused on ALD as a deposition route to promote denser, more conformed, uniform, and amorphous Al_2O_3 films to stall the Fe (and Ni) diffusion. Their data suggests a similar blockage effect of the ALD-grown barrier, at one-third thicknesses compared to their sputtered cousin[129,130]. Later they reported a 95% reduction in Fe and Ni contamination when using 300 nm and 30 nm amorphous Al_2O_3, respectively, compared to no barriers[131]. Details of their ALD process can be found in their earlier publication[129]. To simplify the deposition and reduce costs, HZB worked on spray pyrolysis to fabricate amorphous Al_2O_3 barriers. Their study suggests the necessity of using ethanol in the solution (to achieve smoothness) and rotating the sample under deposition (to achieve compact and homogenous films) to avoid shunt paths and pinholes[127].

Anodization is a scalable, controllable, and relatively simple growth technique explored in the interesting work of Fujifilm and AIST. Moriwaki et al. grew a relatively thick 10 µm Al_2O_3 on top of an even thicker Al laminated SS substrate. Such a bilayer

successfully blocked impurities and insulated the stack with excellent homogeneity and uniformity (± 5%). Moving to sub-module scales and having monolithic integration in mind, their barrier also fared well under the so-called P1 patterning, where the (Mo) back contact is structured. In fact, the dielectric layer did not deteriorate afterwards, and still showed a breakdown voltage of around 500 V, nearly thrice the acceptable range[132].

Lee et al. compared SiOx and intrinsic zinc oxide (i-ZnO) as barriers for co-evaporated CIGS with sodium-doped Mo back contact. Their study suggests ZnO's superiority through more optimized Na distribution after the absorber growth. This is then reasonably attributed to ZnO's higher thermal conductivity, providing a higher thermal budget for CIGS synthesis[133]. The suitability of i-ZnO as a barrier layer is also studied by others using co-evaporation for CIGS growth[134,135].

As hinted initially, such conclusions cannot be readily extended to other CIGS processing temperatures/ techniques. E.g., Ahn et al. found ZnO to be inferior to SiO_x as a barrier layer in sequentially grown Kesterite absorbers. This was attributed to its comparably higher diffusion coefficient and susceptibility in reacting with Se. The latter is reported to result in the formation of a thin ZnSe layer with an even higher diffusion coefficient, which accelerates the outward diffusion of Fe into the absorber. Such discrepancies suggest the necessity of considering the barrier's intrinsic properties and diffusion behavior under a reactive (selenium) atmosphere[121].

SUMMARY AND OUTLOOK

In 2024 CIGS technology celebrates its half-century birthday, with many highs and lows along the way. The (renewable) energy-demanding future does hold a realistic promise for CIGS. Increased interest in space activities, multi-junction tandem configurations, and integrated PV in (mobile) applications with curved surfaces all require properties that are well achieved in this technology. We looked into stainless-steel-based flexible CIGS as a strong contender for such purposes and pointed out the necessity and importance of a diffusion barrier in their fabrication. A wide range of materials used as this layer in the literature were collected, and a summary of their properties and shortcomings was provided.

The literature suggests a need for *tailored* barrier layer material, thicknesses, and deposition methods, depending on the employed CIGS synthesis technique and temperature. In other words, no *one fits all solution* can be singled out. Nonetheless, a rather general trend was seen as follows. Looking at the number of reports, a Cr layer or thickening of Mo back contact in the metallic, SiO_x variations in the oxides, and TiN in nitrides are the most used barriers in the literature. Additionally, for all kinds, depositing a thin Ti layer beneath the barriers seems to improve diffusion blockage and stack integrity by promoting interlayer adhesion. In terms of barrier thickness, in either of the classes, most of the literature indicates a need for hundreds of nanometers, with oxides leaning towards micron thick, and nitrides and metals below half a micron. This means a deposition method like conventional ALD would not be an industrially friendly choice despite its benefits, like film conformity. On the other hand, large-scale, and cost-effective growth techniques that are already part of CIGS technology value chain, such as DC or RF sputtering, are strong contenders. Nevertheless, there is no definitive solution here either, and other methods like evaporation and solution processing also showed efficacy.

In the case of monolithic integration, one must either choose an insulating diffusion barrier or deposit an additional thin insulator film in the stack. In either case, SiO_x and its variations are the most used material. AlOx and ZnO was also shown to be appropriate candidates for this purpose. However, given a need for thick layers to also succeed in impurity blockage, they may come with a risk of delamination, surface defects, and reduced flexibility- which defeats the purpose of technology. Therefore, it might be more practical to turn to other interconnect technologies and avoid the complexities coming with monolithic integration for SS-based CIGS.

Furthermore, a recurring challenge in the literature is the barrier performance in the presence of alkali sources, which cannot be snubbed when aiming for high-performing devices. We covered different groups' approaches to include light and heavy alkalis, and through different studies, the necessity of simultaneous co-optimization of the alkali inclusion and contamination blockage was emphasized. These elements and Fe have similar diffusion paths through grain boundaries and interact when present at the same time. Therefore, it appears more practical to synthesize the absorber first, focusing on impeding contaminations, and later use PDT to introduce alkalis at comparably lower temperatures where Fe diffusion is less probable.

Received: 21 December 2022; Accepted: 7 July 2023;
Published online: 07 August 2023

REFERENCES

1. Greene, J. E., Sequeda-Osorio, F., Streetman, B. G., Noonan, J. R. & Kirkpatrick, C. G. Measurement of boron impurity profiles in Si using glow discharge optical spectroscopy. *Appl. Phys. Lett.* **25**, 435–438 (1974).
2. Jäger-Waldau, A. Progress in Chalcopyrite Compound Semiconductor Research for Photovoltaic Applications and Transfer of Results into Actual Solar Cell Production. In *Practical Handbook of Photovoltaics* 373–395 (Elsevier, 2012).
3. Green, M. A. et al. Solar cell efficiency tables (Version 60). *Prog. Photovolt. Res. Appl* **30**, 687–701 (2022).
4. Mufti, N. et al. Review of CIGS-based solar cells manufacturing by structural engineering. *Sol. Energy* **207**, 1146–1157 (2020).
5. V. K. Kapur, V. K. Kapur, A. Bansal, & S. Roth. Roadmap for manufacturing cost competitive CIGS modules. In *2012 38th IEEE Photovoltaic Specialists Conference* 003343–003348. https://doi.org/10.1109/PVSC.2012.6318289 (2012).
6. Aghaei, M. et al. Review of degradation and failure phenomena in photovoltaic modules. *Renew. Sust. Energ.* **159**, 112160 (2022).
7. Banik, U. et al. Enhancing passive radiative cooling properties of flexible CIGS solar cells for space applications using single layer silicon oxycarbonitride films. *Sol. Energy Mater. Sol. Cells* **209**, 110456 (2020).
8. Afshari, H. et al. The role of metastability and concentration on the performance of CIGS solar cells under Low-Intensity-Low-Temperature conditions. *Sol. Energy Mater. Sol. Cells* **212**, 110571 (2020).
9. Zajac, K. et al. New findings of the German joint project "flexible CIGSe thin film solar cells for space flight". in *2009 34th IEEE Photovoltaic Specialists Conference (PVSC)* 000055–000059. https://doi.org/10.1109/PVSC.2009.5411749 (2009).
10. Lang, F. et al. Proton Radiation Hardness of Perovskite Tandem Photovoltaics. *Joule* **4**, 1054–1069 (2020).
11. Tiwari, A. N., Krejci, M., Haug, F.-J. & Zogg, H. 12.8% Efficiency Cu(In,Ga)Se2 solar cell on a flexible polymer sheet. *Prog. Photovolt: Res. Appl.* **7**, 393–397 (1999).
12. Carron, R. et al. Heat-light soaking treatments for high-performance CIGS solar cells on flexible substrates. Preprint at https://www.researchsquare.com/article/rs-2116168/v1 (2022).
13. Zortea, L. et al. Cu(In,Ga)Se2 solar cells on low cost mild steel substrates. *Sol. Energy* **175**, 25–30 (2018).
14. Imec claims 24.6% efficiency for tandem CIGS cell based on perovskite. *pv magazine International* https://www.pv-magazine.com/2018/09/26/imec-claims-24-6-efficiency-for-tandem-cigs-cell-based-on-perovskite/.
15. Jošt, M. et al. Perovskite/CIGS Tandem Solar Cells: From Certified 24.2% toward 30% and Beyond. *ACS Energy Lett.* **7**, 1298–1307 (2022).
16. Record breaking 23% efficiency proved for flexible Perovskite/CIGS- tandem. *MiaSolé* http://miasole.com/record-breaking-23-efficiency-proved-for-flexible-perovskite-cigs-tandem/ (2019).
17. New efficiency record for CIGS solar modules. *AVANCIS* https://www.avancis.de/en/avancis-achieves-new-efficiency-record-for-cigs-solar-modules/ (2021).
18. Kainikkara Vatakketath, R. Investigation of the Transparent Conducting Oxide (TCO) material used in CIGS thin film solar cell in Midsummer AB. (Uppsala University, 2020).
19. Sunplugged Photovoltaics. *Sunplugged Photovoltaics* https://sunplugged.at/.
20. Niu, J. et al. Techniques to Achieve Stretchable Photovoltaic Devices from Physically Non-Stretchable Devices through Chemical Thinning and Stress-Releasing Adhesive. *Adv. Opt. Mater.* **10**, 2200844 (2022).

21. Ascent Solar. https://ascentsolar.com/.
22. AVANCIS GmbH. https://www.avancis.de/en.
23. Midsummer - Diskreta svensktillverkade solcellstak. *Midsummer* https://midsummer.se/en/.
24. Miasolé products. *MiaSolé* https://miasole.com/.
25. World record efficiency of 26.5% on a tandem solar cell based on a flexible CIGS solar cell. *Solliance Solar Research* https://www.solliance.eu/2021/world-record-efficiency-on-a-tandem-solar-cell/ (2021).
26. Ruiz-Preciado, M. A. et al. Monolithic Two-Terminal Perovskite/CIS Tandem Solar Cells with Efficiency Approaching 25%. *ACS Energy Lett.* **7**, 2273–2281 (2022).
27. Kohl, T. et al. Bias dependent admittance spectroscopy of thin film solar cells: KF post deposition treatment, accelerated lifetime testing, and their effect on the CVf loss maps. *Sol. Energy Mater. Sol. Cells* **231**, 111289 (2021).
28. Lopes, T. S. et al. On the Importance of Joint Mitigation Strategies for Front, Bulk, and Rear Recombination in Ultrathin Cu(In,Ga)Se $_2$ Solar Cells. *ACS Appl. Mater. Interf.* **13**, 27713–27725 (2021).
29. Feurer, T. Narrow band gap Cu(In,Ga)Se2 for tandem solar cell application. https://doi.org/10.3929/ethz-b-000389221 (ETH Zurich, 2019).
30. Zweibel, K., Ullal, H. S. & Mitchell, R. L. Polycrystalline thin film photovoltaics. In *IEEE Conference on Photovoltaic Specialists* 458–466 vol. 1 (1990).
31. Afshari, H. et al. CIGS Solar Cells for Outer Planetary Space Applications: the Effect of Proton Irradiation. In *2020 47th IEEE Photovoltaic Specialists Conference (PVSC)* 2635–2637. https://doi.org/10.1109/PVSC45281.2020.9300610 (2020).
32. Otte, K., Makhova, L., Braun, A. & Konovalov, I. Flexible Cu(In,Ga)Se2 thin-film solar cells for space application. *Thin Solid Films* **511–512**, 613–622 (2006).
33. Kamikawa, Y., Nishinaga, J., Shibata, H. & Ishizuka, S. Efficient Narrow Band Gap Cu (In, Ga) Se2 Solar Cells with Flat Surface. *ACS Appl. Mater. Interf.* **12**, 45485–45492 (2020).
34. Ochoa, M., Buecheler, S., Tiwari, A. N. & Carron, R. Challenges and opportunities for an efficiency boost of next generation Cu(In,Ga)Se $_2$ solar cells: prospects for a paradigm shift. *Energy Environ. Sci.* **13**, 2047–2055 (2020).
35. Martulli, A. et al. Towards market commercialization: Lifecycle economic and environmental evaluation of scalable perovskite solar cells. *Prog. Photovolt: Res. Appl.* **31**, 180–194 (2022).
36. *Indium Availability for CIGS*. https://cigs-pv.net.
37. Jutteau, S., Guillemoles, J.-F. & Paire, M. Design, prototyping and characterization of micro-concentrated photovoltaic systems based on Cu(In,Ga) Se2 solar cells, Conception, prototypage et caractérisation de microsystèmes systèmes photovoltaïques à concentration à base de cellules solaires Cu (In, Ga) Se2. (Université Pierre et Marie Curie - Paris VI, 2016).
38. Zhang, Y., Kim, M., Wang, L., Verlinden, P. & Hallam, B. Design considerations for multi-terawatt scale manufacturing of existing and future photovoltaic technologies: challenges and opportunities related to silver, indium and bismuth consumption. *Energy Environ. Sci.* **14**, 5587–5610 (2021).
39. Zakutayev, A. et al. Emerging inorganic solar cell efficiency tables (version 2). *J. Phys. Energy* **3**, 032003 (2021).
40. EV-Expert talk: Material sustainability aspects for PV technology | EnergyVille. https://www.energyville.be/en/news-events/ev-expert-talk-material-sustainability-aspects-pv-technology.
41. Indium supply not an issue for CIGS industry. *pv magazine International* https://www.pv-magazine.com/2021/08/11/indium-supply-not-an-issue-for-cigs-industry/.
42. Horowitz, K. A. W., Fu, R. & Woodhouse, M. An analysis of glass–glass CIGS manufacturing costs. *Sol. Energy Mater. Sol. Cells* **154**, 1–10 (2016).
43. Kawakita, S. et al. Lightweight, Flexible and High-Efficiency Cu (In, Ga) Se2 Thin-Film Solar Cells with Lift- off Process. In European Photovoltaic Specialists Conference (EUPVSC) (2012).
44. Nassiri Nazif, K. et al. High-specific-power flexible transition metal dichalcogenide solar cells. *Nat. Commun.* **12**, 7034 (2021).
45. Ishizuka, S., Yoshiyama, T., Mizukoshi, K., Yamada, A. & Niki, S. Monolithically integrated flexible Cu(In,Ga)Se2 solar cell submodules. *Sol. Energy Mater. Sol. Cells* **94**, 2052–2056 (2010).
46. Britt, J. S., Wiedeman, S., Schoop, U. & Verebelyi, D. High-volume manufacturing of flexible and lightweight CIGS solar cells. in *2008 33rd IEEE Photovoltaic Specialists Conference* 1–4. https://doi.org/10.1109/PVSC.2008.4922503 (2008).
47. Akinwande, D., Petrone, N. & Hone, J. Two-dimensional flexible nanoelectronics. *Nat. Commun.* **5**, 1–12 (2014).
48. Herrmann, D. et al. High-Performance Barrier Layers for Flexible CIGS Thin-Film Solar Cells on Metal Foils. *MRS Proc.* **763**, B6.10 (2003).
49. Kampmann, A. et al. Electrodeposition of CIGS on Metal Substrates. *MRS Proc.* **763**, B8.5 (2003).
50. Stanley, M. et al. A comparative study of the impact of Mo and stainless steel substrates on the properties of Cu(In,Ga)Se2 based solar cells. *Thin Solid Films* **671**, 6–11 (2019).
51. Kim, H.-S., Jeong, W.-L. & Lee, D.-S. Earth-Abundant CZTSSe Thin Film Solar Cells on Flexible Stainless Steel Foil Substrates. In *2017 IEEE 44th Photovoltaic Specialist Conference (PVSC)* 1665–1668 https://doi.org/10.1109/PVSC.2017.8366211 (2017).
52. Misra, P. et al. A non-vacuum dip coated SiO2 interface layer for fabricating CIGS solar cells on stainless steel foil substrates. *Sol. Energy* **214**, 471–477 (2021).
53. Wuerz, R. et al. CIGS thin-film solar cells on steel substrates. *Thin Solid Films* **517**, 2415–2418 (2009).
54. Wuerz, R., Eicke, A., Kessler, F. & Pianezzi, F. Influence of iron on the performance of CIGS thin-film solar cells. *Sol. Energy Mater. Sol. Cells* **130**, 107–117 (2014).
55. Herz, K. et al. Dielectric barriers for flexible CIGS solar modules. *Thin Solid Films* **403–404**, 384–389 (2002).
56. Jackson, P., Grabitz, P., Strohm, A., Bilger, G. & Schock, H.-W. Contamination of Cu (in, Ga) Se2 by metallic substrates. in 1936–1938 (2004).
57. Eisenbarth, T., Caballero, R., Kaufmann, C. A., Eicke, A. & Unold, T. Influence of iron on defect concentrations and device performance for Cu(In,Ga)Se2 solar cells on stainless steel substrates. *Prog. Photovolt: Res. Appl.* **20**, 568–574 (2012).
58. Stolwijk, N. A. Obeidi, Sh., Bastek, J., Wuerz, R. & Eicke, A. Fe diffusion in polycrystalline Cu(In,Ga)Se2 layers for thin-film solar cells. *Appl. Phys. Lett.* **96**, 244101 (2010).
59. Lu, H.-T., Yang, C.-Y. & Lu, C.-H. Formation process and photovoltaic properties of Cu(In,Ga)Se2 and (Ag,Cu)(In,Ga)Se2 on flexible stainless steel substrates formed at different selenization temperatures. *J. Mater. Sci: Mater. Electron* **27**, 10642–10649 (2016).
60. Kessler, F., Herrmann, D. & Powalla, M. Approaches to flexible CIGS thin-film solar cells. *Thin Solid Films* **480–481**, 491–498 (2005).
61. Kessler, F. & Rudmann, D. Technological aspects of flexible CIGS solar cells and modules. *Sol. Energy* **77**, 685–695 (2004).
62. Morán, A., Nwakanma, O., Velumani, S. & Castaneda, H. Comparative study of optimised molybdenum back-contact deposition with different barriers (Ti, ZnO) on stainless steel substrate for flexible solar cell application. *J. Mater. Sci: Mater. Electron* **31**, 7524–7538 (2020).
63. Amouzou, D. et al. Adhesion, resistivity and structural, optical properties of molybdenum on steel sheet coated with barrier layer done by sol–gel for CIGS solar cells. *Thin Solid Films* **531**, 535–540 (2013).
64. Ruckh, M. et al. Influence of substrates on the electrical properties of Cu(In,Ga) Se2 thin films. *Sol. Energy Mater. Sol. Cells* **41–42**, 335–343 (1996).
65. Ishizuka, S., Kamikawa, Y. & Nishinaga, J. Lightweight and flexible Cu(In,Ga) Se2 solar minimodules: toward 20% photovoltaic efficiency and beyond. *npj Flex. Electron* **6**, 90 (2022).
66. Salomé, P. M. P., Rodriguez-Alvarez, H. & Sadewasser, S. Incorporation of alkali metals in chalcogenide solar cells. *Sol. Energy Mater. Sol. Cells* **143**, 9–20 (2015).
67. Contreras, M. A. et al. Progress toward 20% efficiency in Cu(In,Ga)Se2 polycrystalline thin-film solar cells. *Prog. Photovolt: Res. Appl.* **7**, 311–316 (1999).
68. Satoh, T., Hashimoto, Y., Shimakawa, S., Hayashi, S. & Negami, T. CIGS solar cells on flexible stainless steel substrates. in *Conference Record of the Twenty-Eighth IEEE Photovoltaic Specialists Conference - 2000 (Cat. No.00CH37036)* 567–570 https://doi.org/10.1109/PVSC.2000.915902 (2000).
69. Jung, D.-Y. et al. Fabrication of in situ alkali doped flexible CIGSSe solar cells by using aqueous spray deposition. *Curr. Appl Phys.* **41**, 66–72 (2022).
70. Jackson, P., Bilger, G., Grabitz, P. & Strohm, A. Metallische Verunreinigungen in Hocheffizienten Cu(In,Ga)Se 2 Solarzellen / Tagung PV-Uni-Netz / Ilmenau / Februar 2005. (2005).
71. Dhere, N. G., Ghongadi, S. R., Pandit, M. B., Jahagirdar, A. H. & Scheiman, D. CIGS2 thin-film solar cells on flexible foils for space power. *Prog. Photovolt: Res. Appl.* **10**, 407–416 (2002).
72. Amouzou, D. Electrical, Optical and Structural Properties Of Functional Multilayers On Steel Sheets For Potential Applications In Cu (In, Ga) Se2 Solar Cells. (University of Namur, 2014).
73. Gao, Z. et al. Study on the performance of Tungsten–Titanium alloy film as a diffusion barrier for iron in a flexible CIGS solar cell. *Sol. Energy* **120**, 357–362 (2015).
74. Kumar, P. & Avasthi, S. Diffusion barrier with 30-fold improved performance using AlCrTaTiZrN high-entropy alloy. *J. Alloy. Compd.* **814**, 151755 (2020).
75. Schöppe, P. et al. Rubidium segregation at random grain boundaries in Cu(In,Ga)Se2 absorbers. *Nano Energy* **42**, 307–313 (2017).
76. Nicoara, N. et al. Direct evidence for grain boundary passivation in Cu(In,Ga) Se2 solar cells through alkali-fluoride post-deposition treatments. *Nat. Commun.* **10**, 3980 (2019).
77. Lee, M. et al. Highly efficient flexible CuIn0.7Ga0.3Se2 solar cells with a thick Na/Mo layer deposited directly on stainless steel. *Appl. Surf. Sci.* **346**, 562–566 (2015).
78. Kim, S.-T. et al. Effect of Na-doped Mo layer as a controllable sodium reservoir and diffusion barrier for flexible Cu(In,Ga)Se2 solar cells. *Energy Rep.* **7**, 2255–2261 (2021).

79. Kim, S.-T. et al. Formation of MoSe2 layer and Ga grading in flexible Cu(In, Ga) Se2 solar cell via Na diffusion. *J. Alloy. Compd.* **899**, 163301 (2022).
80. Choi, P.-P., Cojocaru-Mirédin, O., Wuerz, R. & Raabe, D. Comparative atom probe study of Cu(In,Ga)Se2 thin-film solar cells deposited on soda-lime glass and mild steel substrates. *J. Appl. Phys.* **110**, 124513 (2011).
81. López-Marino, S. et al. Earth-abundant absorber based solar cells onto low weight stainless steel substrate. *Sol. Energy Mater. Sol. Cells* **130**, 347–353 (2014).
82. Khelifi, S. et al. Characterization of flexible thin film CIGSe solar cells grown on different metallic foil substrates. *Energy Procedia* **2**, 109–117 (2010).
83. Platzer-Björkman, C. et al. Diffusion of Fe and Na in co-evaporated Cu(In,Ga)Se2 devices on steel substrates. *Thin Solid Films* **535**, 188–192 (2013).
84. Cho, D.-H. et al. Photovoltaic performance of flexible Cu(In,Ga)Se2 thin-film solar cells with varying Cr impurity barrier thickness. *Curr. Appl Phys.* **13**, 2033–2037 (2013).
85. Hartmann, M. et al. Flexible and light weight substrates for Cu(In,Ga)Se/sub 2/ solar cells and modules. in *Conference Record of the Twenty-Eighth IEEE Photovoltaic Specialists Conference - 2000 (Cat. No.00CH37036)* 638–641 https://doi.org/10.1109/PVSC.2000.915924 (2000).
86. Kaufmann, C. A., Neisser, A., Klenk, R. & Scheer, R. Transfer of Cu(In,Ga)Se2 thin film solar cells to flexible substrates using an in situ process control. *Thin Solid Films* **480–481**, 515–519 (2005).
87. Sun, K. et al. Influence of sodium incorporation on kesterite Cu2ZnSnS4 solar cells fabricated on stainless steel substrates. *Sol. Energy Mater. Sol. Cells* **157**, 565–571 (2016).
88. Sun, K. et al. Flexible kesterite Cu2ZnSnS4 solar cells with sodium-doped molybdenum back contacts on stainless steel substrates. *Sol. Energy Mater. Sol. Cells* **182**, 14–20 (2018).
89. Mansfield, L. M. et al. Sodium-doped molybdenum targets for controllable sodium incorporation in CIGS solar cells. in *2011 37th IEEE Photovoltaic Specialists Conference* 003636–003641. https://doi.org/10.1109/PVSC.2011.6185937 (2011).
90. Jiang, X. et al. Study on the performance of titanium film as a diffusion barrier layer for CIGS solar-cell application on stainless-steel substrates. *Clean. Energy* **3**, 217–221 (2019).
91. Palekis, V., Singh, K., Feng, X., Morel, D. L. & Ferekides, C. S. Diffusion barriers for CdS/CdTe Solar cells fabricated on flexible substrates. In *2013 IEEE 39th Photovoltaic Specialists Conference (PVSC)* 1150–1155. https://doi.org/10.1109/PVSC.2013.6744344 (2013).
92. Kranz, L. et al. Doping of polycrystalline CdTe for high-efficiency solar cells on flexible metal foil. *Nat. Commun.* **4**, 2306 (2013).
93. Sun, B. et al. Enhanced thermal stability of Mo film with low infrared emissivity by a TiN barrier layer. *Appl. Surf. Sci.* **571**, 151368 (2022).
94. Eguchi, R., Yamamuro, H. & Takashiri, M. Enhanced thermoelectric properties of electrodeposited Bi2Te3 thin films using TiN diffusion barrier layer on a stainless-steel substrate and thermal annealing. *Thin Solid Films* **714**, 138356 (2020).
95. Matenoglou, G. M. et al. Optical properties, structural parameters, and bonding of highly textured rocksalt tantalum nitride films. *J. Appl. Phys.* **104**, 124907 (2008).
96. Sun, L. et al. Effect of TiN diffusion barrier layer on residual stress and carrier transport in flexible CZTSSe solar cells. *Ceram* **48**, 19891–19899 (2022).
97. Chen, J. S. Thermal stability of Cu/TiN and Cu/Ti/TiN metallizations on silicon. *Thin Solid Films* ***396***, 205–209 (2001).
98. Messaid, B. E. et al. Optimization of a rear system based on titanium nitride for a flexible CuInSe2 solar cell. *Optik* **206**, 164305 (2020).
99. Liu, W.-S., Hu, H.-C., Pu, N.-W. & Liang, S.-C. Developing flexible CIGS solar cells on stainless steel substrates by using Ti/TiN composite structures as the diffusion barrier layer. *J. Alloy. Compd.* **631**, 146–152 (2015).
100. Kumar, P., Jithin, M. A., Mohan, S. & Avasthi, S. Hundred-fold reduction in Iron diffusivity in titanium nitride diffusion barrier on steel by microstructure engineering. *Thin Solid Films* **716**, 138416 (2020).
101. Li, J., Gao, L. & Guo, J. Mechanical properties and electrical conductivity of TiN–Al2O3 nanocomposites. *J. Eur. Ceram.* **23**, 69–74 (2003).
102. Fujii, R., Gotoh, Y., Liao, M. Y., Tsuji, H. & Ishikawa, J. Work function measurement of transition metal nitride and carbide thin films. *Vacuum* **80**, 832–835 (2006).
103. Halas, S. & Durakiewicz, T. Work functions of elements expressed in terms of the Fermi energy and the density of free electrons. *J. Phys. Condens. Matter* **10**, 10815–10826 (1998).
104. Mahieu, S. et al. Sputter deposited transition metal nitrides as back electrode for CIGS solar cells. *Sol. Energy* **85**, 538–544 (2011).
105. Xiong, J., Gu, H., Hu, K. & Hu, M. Influence of substrate metals on the crystal growth of AlN films. *Int J. Min. Met. Mater.* **17**, 98–103 (2010).
106. Li, B. et al. Barrier effect of AlN film in flexible Cu(In,Ga)Se2 solar cells on stainless steel foil and solar cell. *J. Alloy. Compd.* **627**, 1–6 (2015).
107. Delgado-Sanchez, J.-M. et al. Ceramic Barrier Layers for Flexible Thin Film Solar Cells on Metallic Substrates: A Laboratory Scale Study for Process Optimization and Barrier Layer Properties. *ACS Appl. Mater. Interf.* **6**, 18543–18549 (2014).
108. Song, S., Liu, Y., Mao, D., Ling, H. & Li, M. Diffusion barrier performances of thin Mo, Mo-N and Mo/Mo-N films between Cu and Si. *Thin Solid Films* **476**, 142–147 (2005).
109. Hodges, D. R. Development of CdTe Thin Film Solar Cells on Flexible Foil Substrates. (University of South Florida, 2009).
110. Li, L., Zhang, X., Huang, Y., Yuan, W. & Tang, Y. Investigation on the performance of Mo2N thin film as barrier layer against Fe in the flexible Cu(In,Ga)Se 2 solar cells on stainless steel substrates. *J. Alloy. Compd.* **698**, 194–199 (2017).
111. Nicollian, E. H. & Brews, J. R. MOS (metal oxide semiconductor) physics and technology. (John Wiley & Sons, 2002).
112. Menéndez, M. F. et al. Development of intermediate layer systems for direct deposition of thin film solar cells onto low cost steel substrates. *Sol. Energy* **208**, 738–746 (2020).
113. Lee, S.-J. et al. Improved performance of amorphous Si thin-film solar cells on 430 stainless steel substrate by an electrochemical mechanical polishing process. *J. Alloy. Compd.* **558**, 95–98 (2013).
114. Liang, H. et al. High efficiency CIGSe solar cells by combinatorially sputtered Cu(In,Ga) followed by selenization. In *2012 38th IEEE Photovoltaic Specialists Conference* 003102–003107. https://doi.org/10.1109/PVSC.2012.6318237 (IEEE, 2012).
115. Lee, S.-K. et al. Se interlayer in CIGS absorption layer for solar cell devices. *J. Alloy. Compd.* **633**, 31–36 (2015).
116. Sim, J.-K. et al. Efficiency enhancement of CIGS compound solar cell fabricated using homomorphic thin Cr2O3 diffusion barrier formed on stainless steel substrate. *Appl. Surf. Sci.* **389**, 645–650 (2016).
117. Sim, J.-K. et al. Improvement in the performance of CIGS solar cells by introducing GaN nanowires on the absorber layer. *J. Alloy. Compd.* **779**, 643–647 (2019).
118. Hamtaei, S., Brammertz, G., Meuris, M., Poortmans, J. & Vermang, B. Dominant Processing Factors in Two-Step Fabrication of Pure Sulfide CIGS Absorbers. *Energies* **14**, 4737 (2021).
119. Kim, M. S., Yun, J. H., Yoon, K. H. & Ahn, B. T. Fabrication of Flexible CIGS Solar Cell on Stainless Steel Substrate by co-Evaporation. *Process. SSP* **124–126**, 73–76 (2007).
120. Chung, Y.-D. et al. The thickness effect of SiOx layer in CIGS thin-film solar cells fabricated on stainless-steel substrate. Conference Record of the IEEE Photovoltaic Specialists Conference 003402 https://doi.org/10.1109/PVSC.2010.5614680 (2010).
121. Ahn, K. et al. Flexible high-efficiency CZTSSe solar cells on stainless steel substrates. *J. Mater. Chem. A* **7**, 24891–24899 (2019).
122. Tseng, C.-W. et al. Effects of SiO_x Barrier Layers Deposited by Spray Technique for CIGS Solar Cells on Metallic Substrates. *ECS Trans.* **60**, 1287–1294 (2014).
123. Zhang, C. et al. High efficiency CIGS solar cells on flexible stainless steel substrate with SiO2 diffusion barrier layer. *Sol. Energy* **230**, 1033–1039 (2021).
124. Martinez-Perdiguero, J. et al. Electrical insulation and breakdown properties of SiO2 and Al2O3 thin multilayer films deposited on stainless steel by physical vapor deposition. *Thin Solid Films* **595**, 171–175 (2015).
125. Wuerz, R. et al. CIGS thin-film solar cells and modules on enamelled steel substrates. *Sol. Energy Mater. Sol. Cells* **100**, 132–137 (2012).
126. Powalla, M. et al. CIGS cells and modules with high efficiency on glass and flexible substrates. *IEEE J. Photovol.* **4**, 440–446 (2013).
127. Gledhill, S. et al. Spray pyrolysis of barrier layers for flexible thin film solar cells on steel. *Sol. Energy Mater. Sol. Cells* **95**, 504–509 (2011).
128. Vermang, B., Fjällström, V., Pettersson, J., Salomé, P. & Edoff, M. Development of rear surface passivated Cu(In,Ga)Se2 thin film solar cells with nano-sized local rear point contacts. *Sol. Energy Mater. Sol. Cells* **117**, 505–511 (2013).
129. Park, H. et al. ALD-Grown Al2O3 as a Diffusion Barrier for Stainless Steel Substrates for Flexible Cu (InGa) Se2 Solar Cells. *Mol. Cryst. Liq. Cryst.* **551**, 147–153 (2011).
130. Herz, K., Eicke, A., Kessler, F., Wächter, R. & Powalla, M. Diffusion barriers for CIGS solar cells on metallic substrates. *Thin Solid Films* **431–432**, 392–397 (2003).
131. Bae, D., Kwon, S., Oh, J., Kim, W. K. & Park, H. Investigation of Al2O3 diffusion barrier layer fabricated by atomic layer deposition for flexible Cu (In, Ga) Se2 solar cells. *Renew. Energ.* **55**, 62–68 (2013).
132. Moriwaki, K. et al. Monolithically integrated flexible Cu(In,Ga)Se2 solar cells and submodules using newly developed structure metal foil substrate with a dielectric layer. *Sol. Energy Mater. Sol. Cells* **112**, 106–111 (2013).
133. Lee, W.-J. et al. Na effect on flexible Cu(In,Ga)Se2 photovoltaic cell depending on diffusion barriers (SiOx, i-ZnO) on stainless steel. *Mater. Chem. Phys.* **147**, 783–787 (2014).
134. Kim, C.-W., Kim, H. J., Kim, J. H. & Jeong, C. Characterization of flexible CIGS thin film solar cells on stainless steel with intrinsic ZnO diffusion barriers. *J. Nanosci. Nanotechnol.* **16**, 5124–5127 (2016).
135. Shi, C. Y., Sun, Y., He, Q., Li, F. Y. & Zhao, J. C. Cu(In,Ga)Se2 solar cells on stainless-steel substrates covered with ZnO diffusion barriers. *Sol. Energy Mater. Sol. Cells* **93**, 654–656 (2009).

136. Li, X. et al. Review and perspective of materials for flexible solar cells. *Mater. Today Energy* **1**, 100001 (2021).
137. Palekis, V. et al. Structural properties of CdTe and ZnTe thin films deposited on flexible foil substrates. in *2010 35th IEEE Photovoltaic Specialists Conference* 001960–001963. https://doi.org/10.1109/PVSC.2010.5616690 (IEEE, 2010).
138. Dettmer, E. S., Romenesko, B. M., Charles, H. K., Carkhuff, B. G. & Merrill, D. J. Steady-state thermal conductivity measurements of AlN and SiC substrate materials. *IEEE Trans. Compon. Hybr. Manuf. Technol.* **12**, 543–547 (1989).
139. Wang, K. & Reeber, R. R. Thermal expansion of copper. *High temp. and mater science* **35**, (1996).
140. Review of Progress Toward 20% Efficiency Flexible CIGS Solar Cells and Manufacturing Issues of Solar Modules. *IEEE J. Photovolt.* **3**, 572–580 (2013).
141. Hsu, W. et al. Electron-Selective TiO_2 Contact for Cu(In,Ga)Se_2 Solar Cells. *Sci. Rep.* **5**, 16028 (2015).
142. Lee, J. et al. Effect of Three-Stage Growth Modification on a CIGS Microstructure. *IEEE J. Photovolt.* **6**, 1645–1649 (2016).
143. Dowon, B., Sehan, K., Joonjae, O., Joowon, L. & Wookyoung, K. Fabrication of High Efficiency Flexible CIGS Solar Cell with ZnO Diffusion Barrier on Stainless Steel Substrate. *MRS Proc.* **1324**, mrss11-1324–d18-05 (2011).
144. Li, B.-Y. et al. Preferred orientation of Cu(In,Ga)Se2 thin film deposited on stainless steel substrate. *Prog. Photovolt: Res. Appl.* **21**, 838–848 (2013).
145. Thongkham, W., Pankiew, A., Yoodee, K. & Chatraphorn, S. Enhancing efficiency of Cu (In, Ga) Se2 solar cells on flexible stainless steel foils using NaF co-evaporation. *Sol. Energy* **92**, 189–195 (2013).
146. Satoh, T., Hashimoto, Y., Shimakawa, S., Hayashi, S. & Negami, T. Cu(In,Ga)Se solar cells on stainless steel substrates covered with insulating layers. *Sol. Energy Mater. Sol. Cells* **75**, 65–71 (2003).
147. Kim, K.-B., Kim, M., Lee, H.-C., Park, S.-W. & Jeon, C.-W. Copper indium gallium selenide (CIGS) solar cell devices on steel substrates coated with thick SiO 2 -based insulating material. *Mater. Res. Bull.* **85**, 168–175 (2017).
148. Herrmann, D. et al. Flexible, Monolithically Integrated Cu(In,Ga)Se_2 Thin-Film Solar Modules. *MRS Proc.* **865**, F15.1 (2005).
149. Ochoa, M., Yang, S.-C., Nishiwaki, S., Tiwari, A. N. & Carron, R. Charge Carrier Lifetime Fluctuations and Performance Evaluation of Cu(In,Ga)Se2 Absorbers via Time-Resolved-Photoluminescence Microscopy. *Adv. Energy Mater.* **12**, 2102800 (2022).

ACKNOWLEDGEMENTS

This project has received funding from the European Union's Horizon 2020 research and innovation program under grant agreement No 850937. S.H. acknowledges financial support by the Flanders Research Foundation (FWO)—strategic basic research doctoral grant 1S31922N.

AUTHOR CONTRIBUTIONS

S.H. and G.B. conceptualized the work. S.H. collected the data and wrote the original manuscript. G.B., J.P., and B.V. reviewed and edited the original draft.

COMPETING INTERESTS

The authors declare no competing interests.

ADDITIONAL INFORMATION

Correspondence and requests for materials should be addressed to Sarallah Hamtaei.

Reprints and permission information is available at http://www.nature.com/reprints

Publisher's note Springer Nature remains neutral with regard to jurisdictional claims in published maps and institutional affiliations.